EFFECT OF DIFFERENCE 10-METHACRYLOYLOXYDECYL DIHYDROGEN PHOSPHATE CONCENTRATIONS ON THE SHEAR BOND STRENGTH BETWEEN ZIRCONIA AND COMPOSITE RESIN

KANKASIT TIYAPRIJAYA

A Thesis Submitted to the Graduate School of Naresuan University
in Partial Fulfillment of the Requirements
for the Master of Science Program in Dentistry
2026

EFFECT OF DIFFERENCE 10-METHACRYLOYLOXYDECYL DIHYDROGEN PHOSPHATE CONCENTRATIONS ON THE SHEAR BOND STRENGTH BETWEEN ZIRCONIA AND COMPOSITE RESIN

KANKASIT TIYAPRIJAYA

A Thesis Submitted to the Graduate School of Naresuan University
in Partial Fulfillment of the Requirements
for the Master of Science Program in Dentistry
2026

Thesis entitled " Effect of difference 10-Methacryloyloxydecyl Dihydrogen Phosphate concentrations on the shear bond strength between zirconia and composite resin "
by Kankasit Tiyaprijaya
has been approved by the Graduate School as partial fulfillment of the requirements for the Master of Science Program in Dentistry
of Naresuan University

Oral Defense Committee

..... Chair
(Professor Mansuang Arksornnukit, Ph.D.)

..... Advisor
(Assistant Professor Pornpot Jiangkongkho, Ph.D.)

..... Internal Examiner
(Assistant Professor Jadesada Palasuk, Ph.D.)

..... Internal Examiner
(Yosnarong Sirimethawong, Ph.D.)

Approved

.....
(Associate Professor Prayuth Poowaruttanawiwit, Ph.D.)
Dean of the Graduate School
20 AUG 2026

Title EFFECT OF DIFFERENCE 10-METHACRYLOYLOXYDECYL DIHYDROGEN PHOSPHATE CONCENTRATIONS ON THE SHEAR BOND STRENGTH BETWEEN ZIRCONIA AND COMPOSITE RESIN

Author Kankasit Tiyaprijaya

Advisor Pornpot Jiangkongkho, PhD

Academic paper M.S. Thesis in Master of Science Program in Dentistry, Naresuan University, 2026

Keywords: 10-Methacryloyloxydecyl Dihydrogen Phosphate, Shear bond strength, Zirconia, Composite resin

ABSTRACT

Zirconia ceramics are favored in restorative dentistry for their superior mechanical strength, biocompatibility, and aesthetic properties. However, achieving a durable adhesive bond remains a significant clinical challenge because zirconia lacks a glassy phase and exhibits high chemical stability, which results in resistance to conventional acid etching and silanization. To overcome this, functional phosphate monomers such as 10-methacryloyloxydecyl dihydrogen phosphate (10-MDP) have been utilized to facilitate chemical bonding. 10-MDP promotes adhesion by forming chemical interactions between the zirconia surface and the resin-based cement. Despite its widespread use, the influence of varying 10-MDP concentrations on bond strength and the specific molecular coordination at the interface requires further investigation.

This study therefore evaluated the effect of different 10-MDP concentrations on the shear bond strength between zirconia and composite resin while investigating the underlying chemical bonding mechanisms through spectroscopic analysis.

Methods: Specimens were randomly divided into nine groups (n = 6): seven experimental groups treated with varying concentrations of experimental MDP solutions (2, 4, 6, 8, 10, 12, and 14% v/v in ethanol), a commercial MDP primer positive control

(CMP; Z-Prime™ Plus), and a non-MDP treated primer negative control (NMP). Zirconia surfaces were treated with these MDP solutions prior to bonding with flowable composite resin. Shear bond strength was measured using a universal testing machine. Chemical coordination modes were analyzed using ^{31}P Nuclear Magnetic Resonance (NMR) spectroscopy and Energy-Dispersive X-ray Spectroscopy (EDS) to correlate molecular configurations with SBS data.

Results: Shear bond strength was significantly influenced by MDP concentration, increasing from 2% (7.1 ± 0.4 MPa) to a peak at 10% (11.3 ± 0.8 MPa), followed by a significant decline at 12% (7.6 ± 0.7 MPa) and 14% (7.7 ± 0.8 MPa).^{31}P NMR analysis revealed that these variations correspond to five distinct bonding configurations (S1–S5). The superior performance of the 10% concentration was associated with the highest proportion of the S2 configuration, representing ionically bonded bidentate complexes. In contrast, the reduction in SBS at higher concentrations coincided with a decrease in S2 intensity and the emergence of S3 (bridging) and S4/S5 (phosphate oligomers).

Conclusions: Bond strength is dictated by the distribution of MDP coordination modes rather than total presence. A 10% concentration is the ideal threshold for maximizing strong S2 ionic bonding. Exceeding this limit promotes non-productive phosphate multilayers that compromise interface stability.

ACKNOWLEDGEMENT

The authors would like to express their gratitude to the Research and Innovation Division, Faculty of Dentistry, Naresuan University, for providing access to the shear bond strength testing and atomic force microscopy facilities. We also thank the Science Lab Centre, Faculty of Science, Naresuan University, for the field emission scanning electron microscopy and energy-dispersive X-ray spectroscopy. Finally, we acknowledge the Scientific and Technological Research Equipment Centre, Chulalongkorn University, for their assistance with the nuclear magnetic resonance spectroscopy.

Kankasit Tiyaprijaya

LIST OF CONTENTS

LIST OF CONTENTS

LIST OF CONTENTS

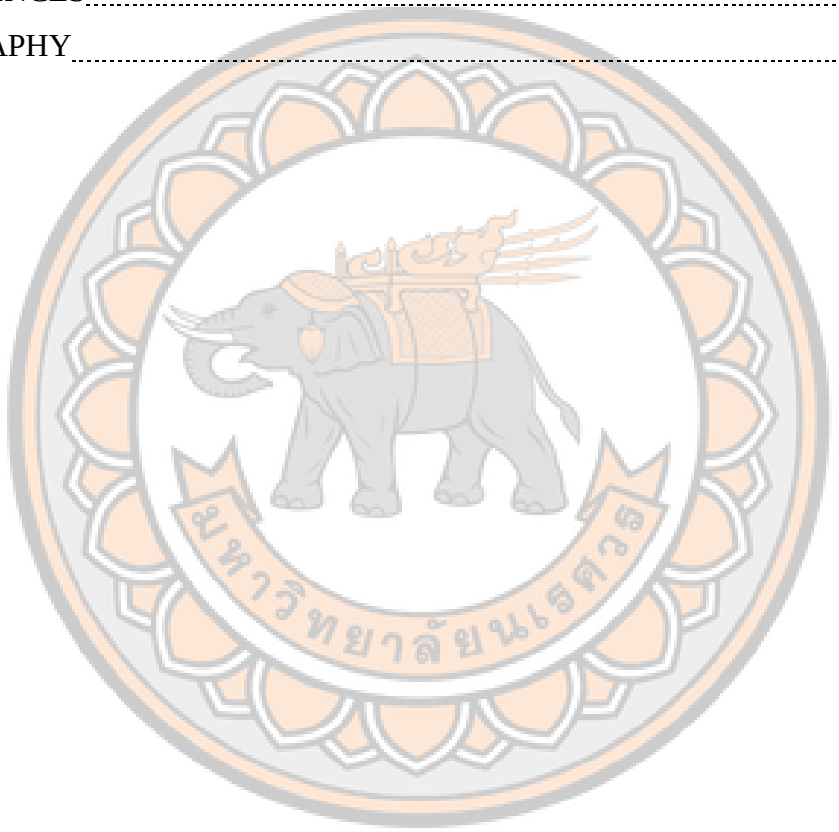

LIST OF TABLES

Page

LIST OF FIGURES

Page

Page

Page

Page

CHAPTER I

INTRODUCTIONS

Background and significant of the study

The evolution of dental materials has a significant transformation from the metals to advanced ceramics. In this decade, zirconia has widely used for dental prostheses over the past few years. Zirconia is excellent mechanical properties, highly biocompatibility and aesthetic appearance. For computer-aided design and computer-aided manufacturing (CAD/CAM) technology, zirconia can be efficient in the workflow. Due to zirconia's strong and inert surface, surface preparation techniques often involve a combination of mechanical and chemical treatments. The most commonly used mechanical surface treatment is air abrasion with alumina particles (Aluminum oxide, Al_2O_3), also known as sandblasting (1). This process increases the surface roughness of zirconia, creating micro-mechanical retention, which can enhance bond strength (2).

Another challenge in working with zirconia is achieving chemical interaction with its surface. Due to its inert nature and the absence of a glass phase, traditional acid-etching techniques are ineffective for surface preparation before adhesive cementation. As a result, establishing a strong chemical bond between zirconia and dental cement during permanent cementation is difficult. One effective approach involves the use of primers containing MDP, which has shown promising results in enhancing the adhesive strength between zirconia and resin cement (3).

Several studies have suggested that MDP can chemically interact with the zirconia surface, forming stable chemical bonds. This interaction enhances the bond strength at the zirconia–resin interface. Therefore, the use of a primer containing MDP prior to the application of an adhesive agent improves the bond strength between zirconia and resin cement. This improvement is attributed to the chemical bonding at the interface, which results in significantly higher bond strength compared to using the adhesive agent alone (4,5).

There are various techniques used to investigate chemical bonding. Nuclear Magnetic Resonance (NMR) spectroscopy provides information on the chemical environment of atoms and detects chemical shifts and splitting patterns, which are useful for investigating the type and nature of chemical bonding (6,7).

The NMR spectroscopy was used to investigate and confirm the chemical interaction mechanism of MDP with zirconia. Significant chemical shifts observed in the ^{31}P NMR spectra indicated that the MDP monomer interacts with the hydrated surface layer of zirconia particles. The identified chemical interactions included hydrogen bonding, formed between the P–OH groups and either zirconium dioxide or another phosphate group, and ionic bonding between the deprotonated $P–O^-$ anions and the positively charged Zr^{4+} ions (8).

Another factor that affects bond strength is the concentration of MDP in the primer agent (9). The higher the number of free phosphate groups in the MDP solution, the greater the potential for chemical interaction. Therefore, the concentration of MDP is directly related to the bond strength achieved (10). Several studies have investigated the effect of varying MDP concentrations to determine the optimal level for maximizing the bond strength between zirconia and resin cement. Previous study reported that a primer containing 4.0 wt% MDP resulted in the highest tensile bond strength compared to other concentrations tested (0.5, 1.0, 2.0, 3.0, and 5.0 wt%) as well as a commercial ceramic primer containing both MDP and a silane coupling agent (11). Another study found that the shear bond strength between zirconia and methacrylate resin showed no significant differences among experimental primer groups containing 10, 15, 20, and 30 wt% MDP. However, all of these groups demonstrated significantly higher shear bond strength compared to the group with 5 wt% MDP (12).

MDP primer appears to be a crucial factor for the chemical bonding interaction between zirconia and resin cement (13). However, the optimal concentration of MDP in primer for achieving the highest bond strength remains unclear. This study aims to enhance the understanding of the optimal MDP concentration that influences the shear bond strength between zirconia and composite resin.

Therefore, the objectives of this study were to investigate the shear bond strength of difference MDP concentrations between zirconia and composite resin. Additionally, it seeks to clarify the chemical bond mechanism between zirconia and composite resin and the molecular structure of the functional groups of MDP.

Research purposes

1. To investigate the effects of concentration of MDP on shear bond strength between the zirconia and the composite resin.

2. To clarify chemical bond between the zirconia and the composite resin.

Research hypothesis

The null hypothesis of the study is H0: There will be no significant difference on the various concentration of MDP on the shear bond strength between zirconia and the composite resin.

CHAPTER II

LITERATURE REVIEW

Zirconia characteristic

Zirconia, or zirconium oxide, is a white crystalline oxide of zirconium that exists in three phases: monoclinic, cubic, and tetragonal. At room temperature, zirconia is typically in the monoclinic phase. When heated, it transforms into the tetragonal phase and subsequently into the cubic phase. Upon cooling, zirconia reverts to the monoclinic phase. This phase transformation involves a rearrangement of the microstructure, leading to changes in mechanical properties, such as dimensions and strength.

In dental applications, tetragonal phase zirconia is preferred due to its appropriate strength, good appearance, and stability. The preparation of zirconia involves heating the monoclinic phase zirconia until it transforms into the tetragonal phase (within a temperature range of 1170 –2370°C) and then stabilizing it in that phase for use. Various stabilizers can be used, such as Yttria (Y_2O_3), Ceria (CeO_2), Calcia (CaO), and Magnesia (MgO). The most common stabilizer used in dental applications is Yttria (Y_2O_3), resulting in Yttria-Stabilized Zirconia (YSZ) or Yttria- Stabilized Tetragonal Zirconia Polycrystal (Y-TZP).

The amount of Yttria used to stabilize zirconia affects the mechanical properties of the product. A higher Yttria com position decreases the ratio of crystalline structure zirconia, resulting in a more translucent appearance but lower mechanical properties. Conversely, lower Yttria content results in a more opaque product with better mechanical properties. Y-TZP is commonly categorized based on the mole percent of Yttria, such as 3Y-TZP (3 mole % Yttria), 4Y-TZP (4 mole % Yttria), 5Y -TZP (5 mole% Yttria), and 6 Y -T Z P (6 mole % Yttria). Some manufacturers combine these into multilayer zirconia, which offers varying levels of translucency and improved aesthetics suitable for dental use.

Today, zirconia is widely used in dentistry as a material for fixed dental prostheses. Due to its excellent properties, zirconia has increasingly replaced full metal and porcelain-fused-to-metal (PFM) restorations. The mechanical properties of zirconia includes 6.05 g/cm3 of density, 1200 HV of hardness, 900-1200 MPa of bend strength, 2000 MPa of

compressive strength, 7-10 MPam1/2 of fracture toughness, 210 GPa of Young's modulus and 11×10-6 1/K of thermal expansion coefficient.

Bonding of zirconia

The long-term clinical success of zirconia restorations depends on the bonding mechanism and cementation that provide high and durable bond strengths. Factors such as ceramic wettability, surface roughness, and coupling agent compositions are crucial for achieving a strong bond between resin cement and zirconia. However, achieving clinical success in zirconia restorations remains a significant challenge, primarily due to the difficulties in adhering to the substrate.

Zirconia's inherent resistance to conventional bonding methods presents a major challenge. Unlike other ceramics, zirconia lacks a glassy phase, making traditional etching techniques, such as hydrofluoric acid etching, ineffective. The recommended approach for bonding to zirconia includes using airborne -particle abrasion (also known as sandblasting) with 50 μm Al_2O_3 at 0.10 to 0.25 MPa in combination with a phosphate monomer-containing adhesive resin.

Chen Y. et al. (12) have reported that air abrasion combined with treatment using methacryloyloxy-decyl-dihydrogen-phosphate (MDP) products results in high chemical affinity and bond strength values. Air abrasion increases the surface area and creates micro-retentions, which improves the mechanical bond of the adhesive resin. MDP-based primers are used to create a chemical bond. The functional monomer MDP has been documented to chemically bond with zirconia. Although several studies have attempted to explore the interactions between MDP and zirconia, there is little evidence of the chemical reactions involved.

The structure of 10-MDP includes a methacrylate group at one end, which can co-polymerize with resin-based cements, and a phosphate group at the other end, which has a strong affinity for metal oxides, including zirconia. A previous study revealed that the 10-MDP monomer can be adsorbed onto zirconia particles through hydrogen bonding between the P=O and Zr-OH groups or via ionic interactions between partially positive Zr and deprotonated MDP (P -O^-). Primers and resin cements containing MDP have shown high

bond strength and durability. While some studies have evaluated the bond strength of adhesives containing different concentrations of MDP to zirconia, the data remain inconclusive, and the optimal concentration of MDP for adhesive systems has not yet been established.

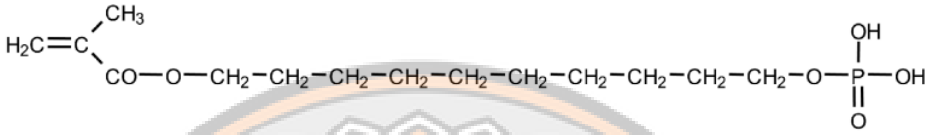

Figure 1 Chemical structure of 10-methacryloxydecyl dihydrogen phosphate (10-MDP)

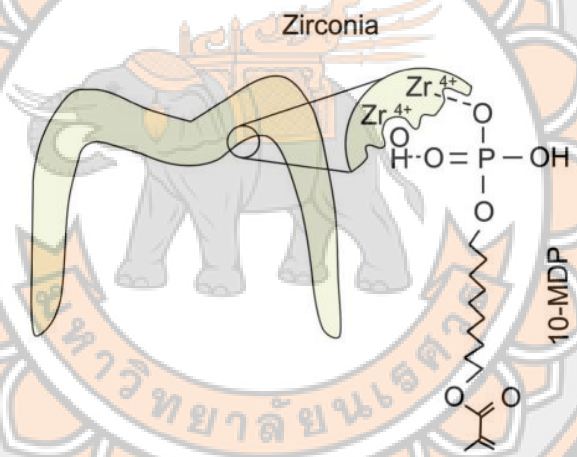

Figure 2 Chemical interaction of the 10-MDP monomer between 10-MDP and zirconia

Shear bond strength

Shear bond strength (SBS) is a measure of the adhesion between two materials, typically used in dentistry and materials science. It quantifies the force required to slide one material parallel to the surface of another material, effectively testing how well they are bonded together.

In dentistry, SBS is particularly important for determining the effectiveness of adhesives in bonding dental materials, such as to enamel or dentin. During the test, a load

is applied to the bonded interface until the bond fails. The force at the point of failure is then divided by the bonded area to calculate the shear bond strength, which is typically expressed in megapascals (MPa).

A high shear bond strength indicates a strong adhesive bond, which is crucial for the longevity and durability of dental restorations like fillings, crowns, and veneers.

Mode of failure

The mode of failure refers to the way in which a bonded material fails when subjected to stress, such as in a shear bond test. Understanding the mode of failure is crucial for evaluating the quality and reliability of the bond between materials. There are generally three primary modes of failure:

Adhesive Failure

The bond fails at the interface between the two materials. This suggests that the adhesive did not adequately bond to one or both surfaces. In other words, the adhesive does not sufficiently stick to one or both surfaces. This type of failure highlights issues with the bonding process, such as improper surface preparation, inadequate adhesive application, or material incompatibility.

Cohesive Failure

The bond fails within one of the materials, rather than at the interface. This type of failure indicates that the adhesive bond is stronger than the internal strength of one of the materials. It may suggest that the adhesive is performing well, but the material itself is the weak link. The material that fails will exhibit tearing, cracking, or other signs of internal disruption, while the other material and the adhesive layer often remain intact.

Mixed Failure

The bond exhibits both adhesive and cohesive failure characteristics. This type of failure suggests a combination of factors affecting both the bond interface and the material itself. It might indicate a partial weakness in the adhesive and/or the bonded materials.

Field Emission Scanning Electron Microscope

A Field Emission Scanning Electron Microscope (FE-SEM) is an enhanced version of the traditional scanning electron microscope (SEM), utilizing a field emission gun (FEG) as its electron source. This innovation provides superior resolution and imaging performance compared to standard thermionic SEMs, making it an essential instrument for detailed material and surface analysis.

The Field Emission Scanning Electron Microscope (FE-SEM) is a highly advanced imaging tool that utilizes a field emission gun (FEG) to generate a focused, high-brightness electron beam, allowing for superior resolution down to the sub-nanometer level. Its exceptional imaging capabilities are complemented by the ability to operate at low accelerating voltages (typically 0.5–5 kV), minimizing damage to delicate or non-conductive samples while enhancing contrast. With a wide depth of field, FE-SEM maintains focus on irregularly shaped surfaces, making it ideal for 3D topographic imaging. It offers versatility through secondary electron imaging for detailed surface morphology, backscattered electron imaging for compositional contrast, and integration with energy-dispersive X-ray spectroscopy (EDS/EDX) for elemental analysis. These features make FE-SEM indispensable for high-resolution studies in fields ranging from nanotechnology to materials science.

Energy-Dispersive X-ray Spectroscopy

Energy-Dispersive X-ray Spectroscopy (EDS or EDX) is an analytical technique commonly used alongside electron microscopy, such as FE-SEM, to identify and quantify a sample's elemental composition. It operates by analyzing the characteristic X-rays emitted by elements when their atoms are excited by an electron beam.

Energy-Dispersive X-ray Spectroscopy (EDS) works by analyzing the characteristic X-rays emitted when an electron beam interacts with a sample. As the beam strikes the sample, electrons from inner atomic shells are ejected, creating vacancies that are filled by electrons from higher energy shells. This transition releases energy in the form of X-rays unique to each element, acting as a fingerprint for elemental identification. These X-rays are detected using specialized devices, such as silicon drift detectors (SDDs), which measure their energy and intensity. The collected data is then processed by the EDS system to generate an elemental spectrum or map, enabling detailed compositional analysis.

Energy-Dispersive X-ray Spectroscopy (EDS) offers several capabilities for analyzing the elemental composition of materials. It enables elemental identification by detecting the characteristic X-ray peaks unique to each element, allowing precise determination of the elements present in a sample. Additionally, EDS provides quantitative analysis, estimating the concentration of these elements in terms of atomic or weight percentages. Elemental mapping is another powerful feature, producing spatial distributions that reveal how elements are distributed across the sample's surface. Furthermore, line scanning allows detailed analysis of elemental composition along a specific line, making EDS a versatile tool for comprehensive material characterization.

Nuclear Magnetic Resonance (NMR)

Nuclear Magnetic Resonance (NMR) is a sophisticated analytical technique used to determine the structure of organic compounds, study molecular dynamics, and investigate the chemical environment of nuclei in a molecule. NMR is widely used in chemistry, biochemistry, and materials science due to its ability to provide detailed information about the atomic-level structure of a substance.

Certain nuclei, such as hydrogen-1 (^{1}H) and carbon-13 (^{13}C), possess a property called spin, which makes them behave like tiny magnets. When placed in an external magnetic field, these nuclear spins align with or against the field, creating different energy levels. Nuclei in the lower energy state can be excited to a higher energy state by applying a radiofrequency (RF) pulse at the correct frequency (the Larmor frequency). When they

relax back to the lower energy state, they emit RF radiation, which is detected as the NMR signal.

The position of the NMR signal is measured in parts per million (ppm) relative to a reference compound (usually TMS, tetramethyl silane). The chemical shift provides information about the electronic environment surrounding the nucleus. NMR signals can split into multiple peaks due to spin-spin coupling with neighboring nuclei. The pattern of splitting (singlet, doublet, triplet, etc.) reveals information about the number of adjacent nuclei. The area under the peaks corresponds to the number of nuclei contributing to that signal, allowing quantification of different groups within a molecule. The distance between split peaks, measured in Hertz (Hz), gives the coupling constant, which provides additional structural information.

The most common type of NMR is ^{1}H NMR (Proton NMR), used to study the hydrogen atoms in a molecule. It provides detailed information about the hydrogen-containing functional groups, their environment, and interactions. The second type is ^{13}C NMR, which focuses on carbon atoms and provides information about the carbon backbone of organic compounds. While it is less sensitive than ^{1}H NMR, it is crucial for studying the structure of carbon-containing compounds. The third type is Solid-State NMR, which is used to study materials in the solid phase, such as polymers, crystals, and complex biological samples. It is particularly useful for investigating non-crystalline or poorly soluble samples. The last type is 2D NMR (Two-Dimensional NMR), which includes techniques like COSY, HSQC, and NOESY. These techniques provide correlations between different nuclei, enabling more complex structural analysis.

The applications of NMR include determining the structure of organic molecules, such as natural products, pharmaceuticals, and polymers, which is known as structural elucidation. It also provides information about the three-dimensional structure of molecules, including proteins and nucleic acids, in solution, referred to as conformational analysis. NMR is used to study molecular dynamics, including diffusion, rotation, and exchange processes, offering insights into the behavior of molecules over time. Additionally, NMR is employed to identify and quantify metabolites in biological samples,

providing insights into metabolic pathways and disease states. Lastly, it is used to study the structure and dynamics of materials, including glasses, ceramics, and polymers.

Sample size and grouping

The sample size of zirconia (KATANA™ Zirconia YML) specimens will be calculated from the software (G*power software version 3.1.9.2, Franz Faul, Universität Kiel, Germany). The level of significance, the type II error (β), the power of estimation was set at 5 percentages (that is P-value = 0.05).

CHAPTER III

RESEARCH METHODOLOGY

Part I: The difference of MDP concentrations

1. MDP primer and solutions

The MDP primer, solutions, ceramic, and materials used in the present study and their manufacturer are shown in Table 1.

Materials	Concentrations	Code	Brand	Mfg.	Batch No.	Composition (%)
MDP Primer						
10-Methacryloyloxydecryl Dihidrogen Phosphate	82.8	MDP	PCM Products GmbH	PCM Products GmbH, Krefeld, Germany	11022206	10-MDP 82.8%
Solutions						
Ethanol	99.9	ETH	RCI Labscan	RCI Labscan Ltd, Bangkok, Thailand	17100329	ETH 99.9%
Ethanol-d6 for NMR, anhydrous	99.8 99 atom%D	d-ETH	RCI Labscan	RCI Labscan Ltd, Bangkok, Thailand	A0434198	d-ETH 99 atom %D
Ceramic						
Zirconia	96.0		KATANA™ Zirconia UTML	Kuraray Noritake, Okayama, Japan	ESHHD	Zirconium oxide, Hafnium oxide, Yttrium oxide, other oxides and pigments
Materials						
Commercial MDP primer		CZP	Z-Prime™ Plus	BISCO, Inc, Schaumburg, IL , USA	2400002418	10-MDP, Ethanol, Bis-GMA, 2-Hydroxyethyl Methacrylate, Triethylamine
Adhesive agent			Single Bond 2 adhesive	3M™ ESPE, MN, USA	10460900	Dimethacrylate resins HEMA, Methacrylate-modified polyalkenoic acid copolymer, Filler Ethanol, Water, Initiators
Flowable composite resin			Filtek™ Supreme Flowable Restorative	3M™ ESPE, MN, USA	10497058	Bis-GMA, TEGDMA, Procrylat, fillers and inorganic fillers

Table 1 Methacryloyloxydecyl dihydrogen phosphate, solutions, ceramic, and materials used in this study and their manufacturer

2. Preparation of zirconia specimens

Specimen design

The specimen template will be designed using the Microsoft 3D Builder program (Microsoft, Redmond, Washington, USA), which allows for the free design, construction, editing, and modification of 3D models (Figure 3). The finalized specimen models will be exported in STL format for subsequent use in computer-aided manufacturing. Each specimen will be prepared in a coin-shaped form, with dimensions of 10 mm in diameter and 3 mm in thickness.

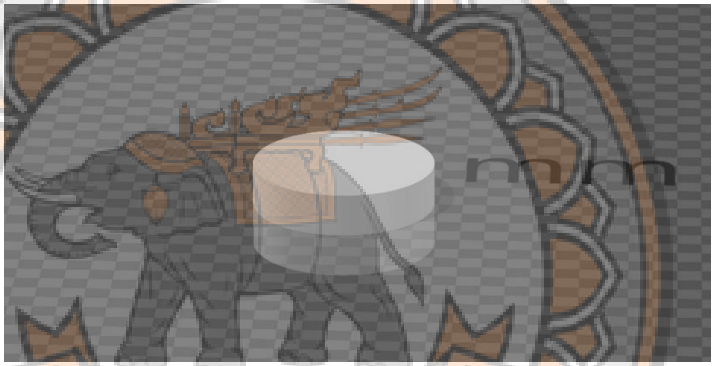

Figure 3 The design of specimen in 3D builder Microsoft program

Specimens Preparation

The specimen template was designed using Microsoft 3D Builder (Microsoft, Redmond, WA, USA). Zirconia specimens—cylindrical in shape with a 10.0 mm diameter and 3.0 mm thickness—were fabricated from zirconia discs (KATANA™ Zirconia UTML, Kuraray Noritake Dental, Okayama, Japan) (Figure 4) using a dry milling machine (DGSHAPE DWX-52D Plus, Roland DG Corporation, Irvine, CA, USA) (Figure 5). Following the milling process (Figure 6), the specimens were sintered in a high-temperature furnace (VITA ZYRCOMAT® 6100 MS, VITA Zahnfabrik, Yorba Linda, CA, USA) (Figure 7-10) according to the manufacturer's recommended protocol (Figure 11). Following the completion of the sintering and cooling cycles, the zirconia specimens were removed from the furnace for the subsequent procedures (Figure 12).

Figure 4 The high translucent zirconia

Figure 5 The computer-aided manufacturing machine

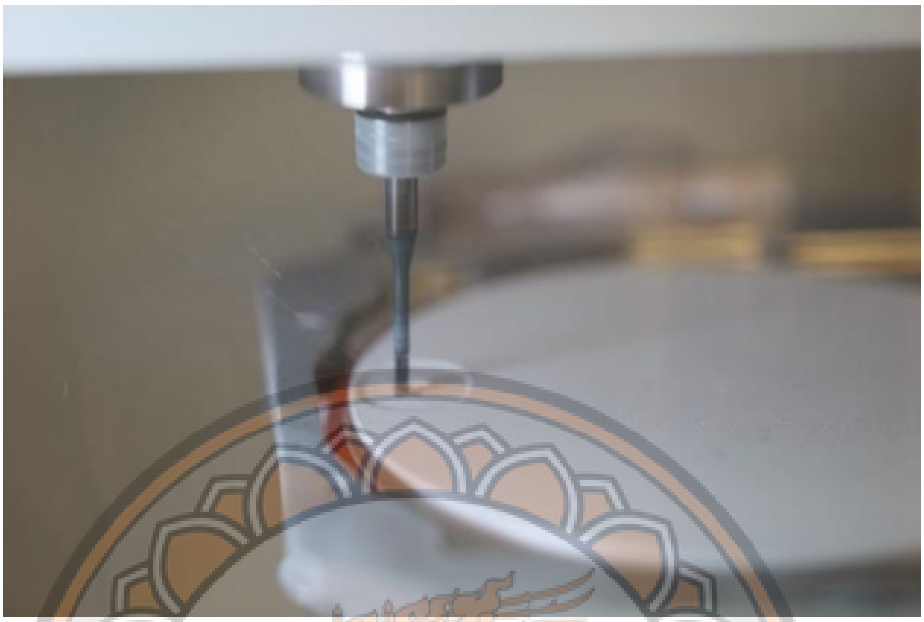

Figure 6 The milling process of computer-aided manufacturing machine

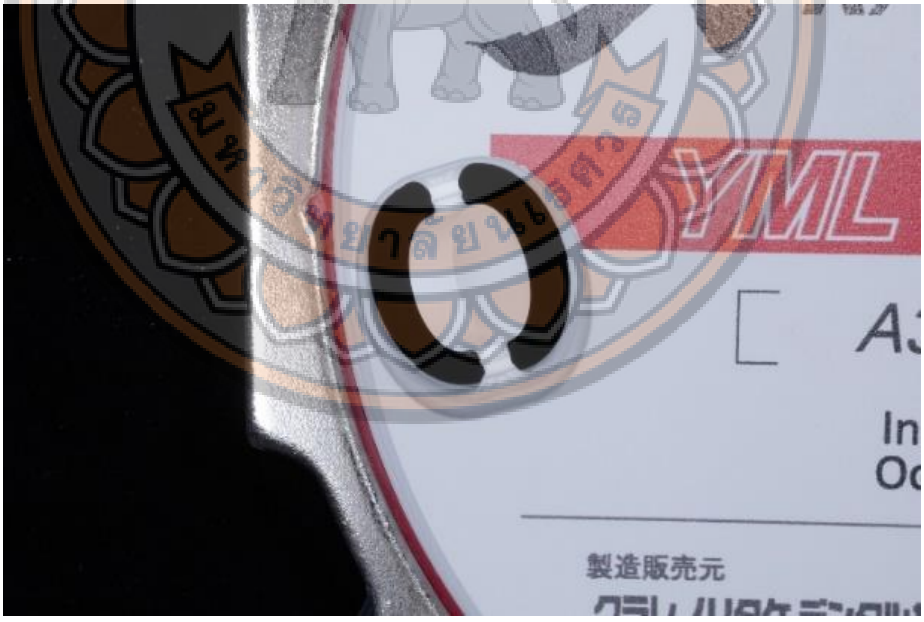

Figure 7 The high translucent zirconia after milling process

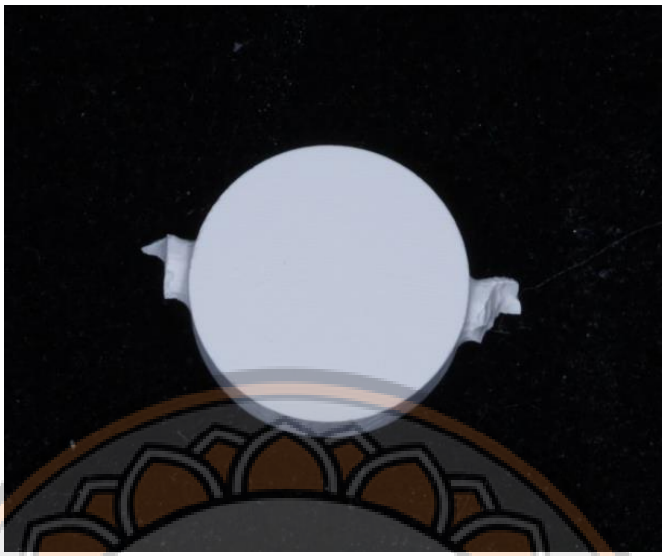

Figure 8 The sectioned zirconia specimen before sintering

Figure 9 The presintered zirconia specimen prepared for sintering in the furnance

Figure 10 The sintering furnance

Figure 11 The temperature sintering protocol

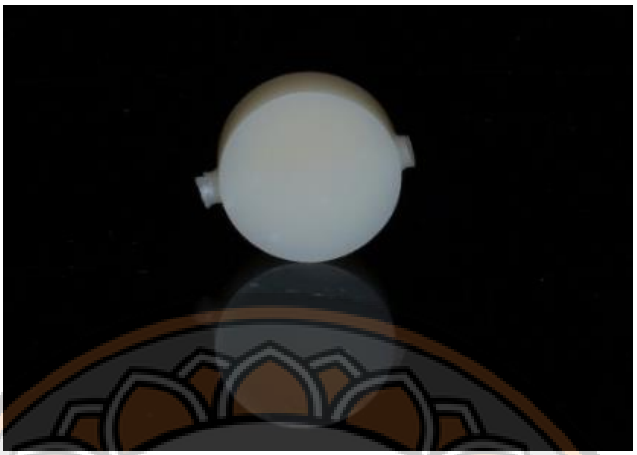

Figure 12 The zirconia disc specimens after sintering

After sintering, the surface of the zirconia specimens was treated using a sandblasting technique with 110 μm aluminum oxide particles for 10 seconds at a pressure of 2 bar, maintaining a distance of 10 mm from the surface for each specimen (Figure 13) (14). Following sandblasting, the specimens were cleaned using a high-pressure steam cleaner, and then further cleaned in an ultrasonic device (BANDELIN electronic GmbH & Co. KG, Heinrichstraße 3–4, Berlin, Germany) for 5 minutes.

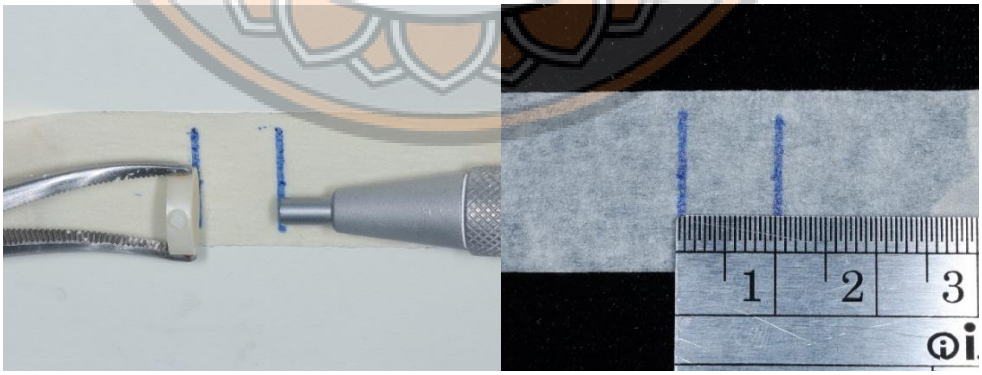

Figure 13 The sandblasting procedure

The surface roughness (Ra) of the zirconia specimens was measured using atomic force microscopy (AFM) in tapping mode (Flex-Axiom; Nanosurf, Liestal, Switzerland) (Figure 14). Twenty-one out of fifty-four zirconia specimens were randomly selected as representative samples to analyze the distribution of surface roughness following the sandblasting procedure. Ra values were calculated using C3000 Control Software, Version 3.5 (Nanosurf, Liestal, Switzerland), based on measurements taken at three central points on each specimen to determine the mean Ra value per specimen (Figure 15). One-way ANOVA will be performed to analyze the mean Ra values across all specimens. Specimens with no statistically significant difference in Ra values will be accepted for use in the experimental group.

Figure 14 The surface roughness (Ra) measurement with an atomic force microscopy (AFM)

Figure 15 The three areas of Zirconia specimen will be identified around the center area for AFM.

The zirconia specimens were mounted in polyvinyl chloride (PVC) cylindrical molds (20 mm in height and 15 mm in diameter) using auto-polymerizing acrylic resin (Fast Curing Custom Tray Acrylic Resin; Instant Tray Mix, Lang Dental Manufacturing Company, IL, USA) (Figure 16). The diameter of the PVC molds was designed to fit the holder of the universal testing machine, which was used to perform the shear bond strength test.

Figure 16 The zirconia specimens were placed into polyvinylchloride cylindrical mold (20.0x15.0 mm) and fixed with auto-polymerized acrylic resin

All specimens will be cleaned using an ultrasonic device (BANDELIN electronic GmbH&Co.KG, Heinrichstraße 3-4, Berlin, Germany) for 5 minutes (Figure 17). To define the surface treatment area of the zirconia disc specimens, a 5.0 mm hole of double-sided adhesive tape (Scotch® Professional Grade Vinyl Electrical Tape Super 88, 3M ESPE, MN, USA) will be placed at the center of each specimen (Figure 18).

Figure 17 An ultrasonic device

Figure 18 The surface treatment area of zirconia specimen

3. Population and sample

The sample size was determined using G*Power software (version 3.1.9.2; Franz Faul, Universität Kiel, Germany) based on data from a previous pilot study. The parameters used for the calculation were as follows: a power (1 - beta error probability) of 0.90 and an alpha (alpha) level of 0.05. The calculation indicated a minimum sample size of 5; however, to ensure statistical power and reliability, a sample size of 6 specimens per group was selected for this study (Figure 19).

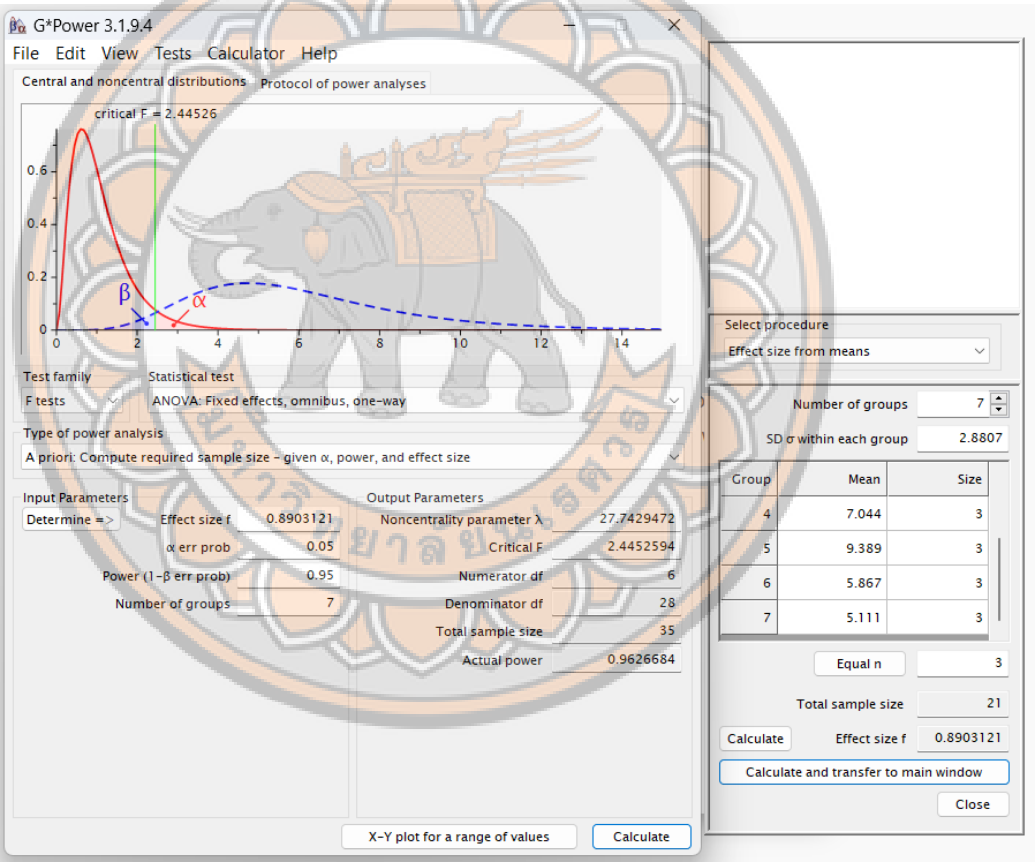

Figure 19 The calculation of sample size by G*Power software using the data from the pilot study

Fifty-four zirconia specimens were randomly divided into 9 groups (*n*=6). Seven groups for the difference experimental MDP concentrations (2, 4, 6, 8, 10, 12, and 14%v/v) commercial MDP primer (CMP), and non-MDP primer (NMP) groups that served as a control.

4. Preparation of experimental MDP

Various concentrations of experimental MDP were prepared by diluting MDP monomer (PCM Products GmbH, Krefeld, Germany) to 2%, 4%, 6%, 8%, 10%, 12%, and 14%v/v in ethanol 99.9%v/v (ETH; RCI Labscan, RCI Labscan Ltd., Bangkok, Thailand). The dilutions were performed using a micropipette (PIPETMAN®, Gilson Inc., Middleton, WI, USA) and homogenized using a vortex mixer (VX100, GIBTHAI Co., Ltd., Bangkok, Thailand) for 10 minutes. The preparation details for each experimental MDP concentration are summarized in Table 2.

The concentration of experimental MDP (% v/v)	MDP (mL)	Ethanol (mL)	Total volume (mL)
2	0.08	3.92	4.00
4	0.16	3.84	4.00
6	0.24	3.76	4.00
8	0.32	3.68	4.00
10	0.40	3.60	4.00
12	0.48	3.52	4.00
14	0.56	3.44	4.00

Table 2 The formulation and preparation of experimental 10-MDP solutions at varying concentrations

5. Surface treatment

Zirconia specimens

The zirconia specimens were rinsed with deionized water for 15 seconds and air-dried using a triple syringe.

For the experimental MDP groups, the 25 microliters of each MDP concentration was applied to the bonding area using a micropipette (Pipetman® Classic, Gilson Inc., Middleton, WI, USA) (Figure 20) and actively agitated with a micro-brush. This was followed by air-drying for 30 seconds until the surface was completely dry at room temperature.

Figure 20 The micropipettes

For the CMP group, a commercial zirconia primer (Z-Prime™ Plus, Bisco, Schaumburg, IL, USA) (Figure 21) was applied to the specimen surfaces following the manufacturer's instructions.

Figure 21 The commercial zirconia primer

The NMP group did not apply the MDP primer.

Adhesive agent

The adhesive agent (Adper™ Single Bond 2, 3M ESPE, St. Paul, MN, USA) (Figure 22) was applied to the bonding area of the zirconia specimens and air-dried to create a thin, uniform film. The adhesive layer was then polymerized using an LED light-curing unit (Elipar™ S10, 3M ESPE; light intensity: 1,200 mW/cm²) for 10 seconds, in accordance with the manufacturer's instructions.

Figure 22 The adhesive agent

Composite resin

The flowable composite resin (Filtek™ Supreme Ultra Flowable Restorative, 3M ESPE, St. Paul, MN, USA) (Figure 23) was injected into a soft polyvinylchloride mold (5.0 mm in diameter and 3.0 mm in height) positioned to another sticky side of the adhesive tape over the treated bonding area (Figure 24). The composite was then light-activated for 20 seconds per section using an LED light-curing unit, utilizing five overlapping irradiation points (four around the periphery and one on the top) to ensure complete polymerization of the specimen (Figure 25).

Figure 23 The flowable composite resin

Figure 24 The injection of flowable composite resin into a soft polyvinylchloride mold

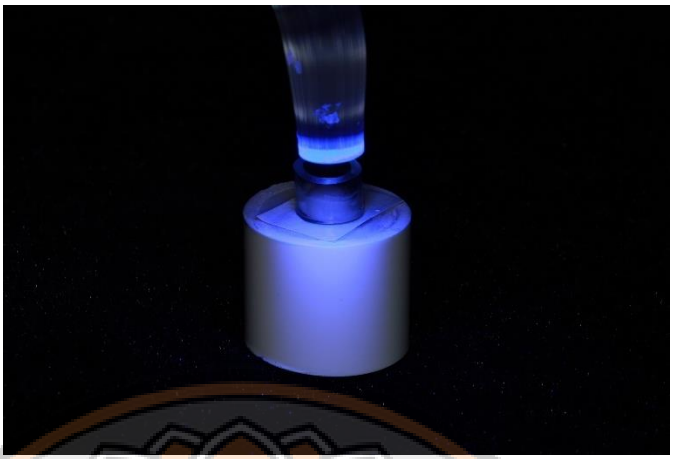

Figure 25 The light activation of flowable composite resin with the LED light-curing unit

6. Thermocycling condition

All zirconia specimens were stored in distilled water at 37 °C for 24 hours prior to thermocycling. Aging was performed in deionized water baths at 5 °C and 55 °C with a dwell time of 30 seconds for 5,000 cycles, using the thermocycling machine (Thermocycler THE 1200, SD Mechatronik GmbH, Bavaria, Germany) (Figure 26) (15,16).

Figure 26 The thermocycling machine

7. Shear bond strength test

The shear bond strength (SBS) test was performed using a universal testing machine (ElectroPlus™ E1000, Instron®, Norwood, MA, USA) (Figure 27) at a crosshead speed of 0.5 mm/min. The specimens were positioned in a specialized shear bond jig to align a chisel-shaped rod from the load cell parallel to the bonding interface (Figure 28). The SBS values were calculated using the system software (Bluehill® Universal, Instron®, Norwood, MA, USA) according to the following equation:

$$\tau = F/A \ (N/mm^2)$$

where, τ = the shear stress (N/mm^2)

F = the force applied (N)

A = the cross-sectional area of material with area parallel to the applied force vector (mm^2)

Figure 27 The universal testing machine

Figure 28 The shear bond strength test

8. Mode of failure analysis

The fracture surfaces of all specimens were examined following the shear bond strength test using a stereomicroscope (Olympus SZX2-ILLT, Olympus Corp., Tokyo, Japan) at 20× magnification. Failure modes were classified into three categories:

1. Adhesive failure: Failure occurring entirely at the interface between the zirconia and the resin cement.
2. Cohesive failure: Failure occurring entirely within the composite resin or the zirconia substrate.
3. Mixed failure: A combination of adhesive failure and cohesive failure within the composite resin.

For specimens exhibiting cohesive failure, the areas of the bonding area and the remaining material were recorded and calculated using ImageJ software (version 1.53k; National Institutes of Health, Bethesda, MD, USA). The mean percentage of cohesive was calculated as follows:

$$\text{The percentage area fracture of Zirconia} = \frac{\text{Area of Zirconia surface fracture}}{\text{The total bonding area of Zirconia surface}} \times 100$$

$$\text{The percentage area fracture of composite resin} = \frac{\text{The composite resin remnants}}{\text{The total bonding area of zirconia surface}} \times 100$$

For the mixed failure mode, the data is typically expressed as ratio that must sum to 100% as follows:

Failure Mode: X% cohesive / Y% adhesive

where, X = the percentage of the cohesive failure

Y = the percentage of the adhesive failure

Part II: Fracture surface topography by field emission scanning electron microscopy (FESEM) and elemental analysis

Surface characterization

Following the shear bond strength test, the fractured surfaces of the zirconia specimens were coated with a thin layer of gold under vacuum using a sputter coater (SPI Sputter Coater, SPI Supplies, West Chester, PA, USA). The surface morphology was examined using a field emission scanning electron microscope (FESEM; Apreo S, Thermo Fisher Scientific, Waltham, MA, USA) (Figure 29) operated at an accelerating voltage of 20 kV. SEM micrographs were obtained at 500× magnification to evaluate the topographical features of the fracture surfaces.

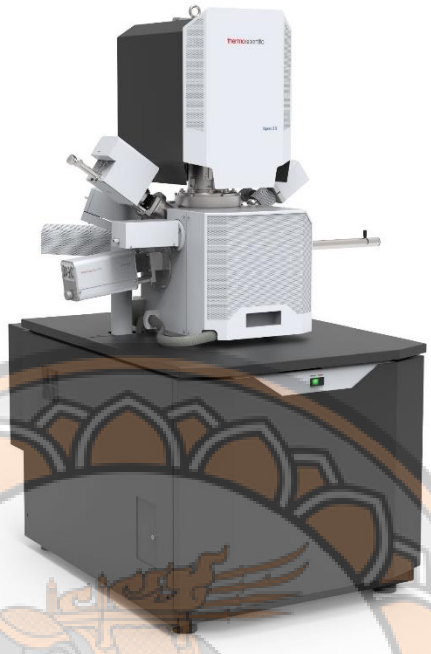

Figure 29 The field emission scanning electron microscope (FESEM)

Elemental analysis

Energy-dispersive X-ray spectroscopy (EDS; ULTIM MAX 65, Oxford Instruments, Abingdon, Oxfordshire, UK) was performed in conjunction with FESEM analysis to verify the presence of MDP on the treated surfaces. This analysis was used to evaluate both the qualitative and quantitative characteristics of the elements on the specimen surfaces. The primary electron beam energy was operated at 20 kV for each specimen. Three distinct areas (each measuring 0.25 × 0.18 mm) at the center of each specimen were examined. The NMP surface was analyzed as a reference.

EDS analysis was employed to identify zirconium (Zr), oxygen (O), and phosphorus (P) on the MDP-treated zirconia surfaces. While zirconium and oxygen were detected on both the NMP and MDP-treated surfaces, phosphorus was detected exclusively on the MDP-treated surfaces. This indicates the presence of phosphate groups from the experimental MDP primer, confirming successful chemical treatment prior to bonding with the flowable composite resin.

Part III: Molecular analysis

NMR spectroscopy

The chemical bonding mechanism between MDP and zirconia was analyzed using solid-state NMR. The sample consisted of a mixture of zirconium oxide (ZrO_2) powder and an experimental MDP solution. Based on representative subgroups that showed no significant differences in shear bond strength, solution concentrations of 2, 4, 10, and 14% v/v were selected.

The ZrO_2 powder was prepared using a milling machine (DGSHAPE DWX-52D Plus, Roland DG Corporation, Irvine, CA, USA) and subsequently filtered through a 190-micron mesh filter (Gerson Elite™ Paint Strainers, The Gerson Companies, Olathe, KS, USA). The particle size distribution and surface area of the powder were determined using a laser particle size distribution analyzer (Partica LA-960V2, HORIBA Advanced Techno Co., Ltd., Fukuoka, Japan) (Figure 30) and an automated gas sorption analyzer (BET method, Anton Paar Ltd., Bangkok, Thailand) (Figure 31), respectively. The optimal volume of the MDP solution applied to the bonding area (circular shape; mean diameter = 4.79 mm; mean area = 18.01 mm^2) was 1.4 µL, resulting in a ratio of 0.077 µL/mm^2 of MDP solution to surface area.

Figure 30 The laser particle size distribution analyzer

Figure 31 The automated gas sorption analyzer

Based on the laser particle size distribution and automated gas sorption analyses, the zirconium oxide powder exhibited a specific surface area of 132.2 m^2/kg (0.132 m^2/g) and a mean particle diameter of approximately 322.8 nm. For a 0.5 g sample of ZrO_2 powder, the optimal volume of the experimental MDP solution was calculated to be 5.082 mL.

A 0.5 g portion of ZrO_2 powder was mixed into 5.0 mL of the 2, 4, 10, and 14% v/v MDP solutions. Each mixture was subjected to ultrasonic agitation for 5 min, followed by static incubation for 20 min to allow for the complete evaporation of the ethanol solvent. This process yielded dry ZrO_2 powder coated with different MDP concentrations. Untreated ZrO_2 powder was prepared separately to serve as a reference.

NMR experiments were conducted using a 400 MHz Fourier Transform Nuclear Magnetic Resonance Spectrometer (FT-NMR; AVANCE III HD/Ascend 400 WB, Bruker Scientific LLC, Billerica, MA, USA) (Figure 32). The ZrO_2 powder and MDP mixtures were examined via solid-state NMR spectroscopy using a 4.0 mm zirconia rotor with a spinning frequency of 10 kHz.

Figure 32 The 400 MHz Fourier Transform Nuclear Magnetic Resonance Spectrometer

Direct polarization ^{31}P NMR spectra were acquired at 162.2 MHz with a pulse length of 3.3 μs (pulse angle of π/2) and a recycle delay of 5 s. Approximately 1,760 pulses were accumulated, using phosphoric acid (H_3PO_4) as an external reference. High-power decoupling was applied during ^{31}P acquisition.

^{1}H NMR spectra were acquired at 400.6 MHz with a pulse length of 3.0 μs (pulse angle of π/4) and a recycle delay of 3 s. Approximately four pulses were accumulated, using adamantane ($C_{10}H_{16}$) as an external reference. For comparison, the ^{1}H NMR spectrum of the untreated ZrO_2 powder and the ^{31}P NMR spectra of all MDP-treated samples were also recorded.

Deconvolution was applied to the ^{31}P NMR spectra to resolve overlapping peaks and ensure accurate chemical shift assignments. Phosphorus nuclei often reside in multiple chemical environments, resulting in closely spaced signals that manifest as broad or merged peaks. Such peaks can be difficult to interpret directly; however, deconvolution allows these

signals to be resolved into individual components. This mathematical approach facilitates the identification of distinct phosphorus species, enables reliable quantitative analysis, and provides a more precise determination of chemical shifts and line shapes.

The molecular structure of the MDP solution was analyzed using liquid-state NMR spectroscopy. ^{31}P NMR spectra were acquired using a 600 MHz Fourier Transform Nuclear Magnetic Resonance Spectrometer (AVANCE NEO Cryoprobe, Bruker Scientific LLC, Billerica, MA, USA) (Figure 33) operating at 25°C. For the ^{31}P measurements, the resonance frequency was 242.93 MHz, with the scan and repetition times set to 10 s. All chemical shifts were referenced to an external phosphoric acid (H_3PO_4) solution. The 10% MDP solution was prepared following the same methodology described in Part I.

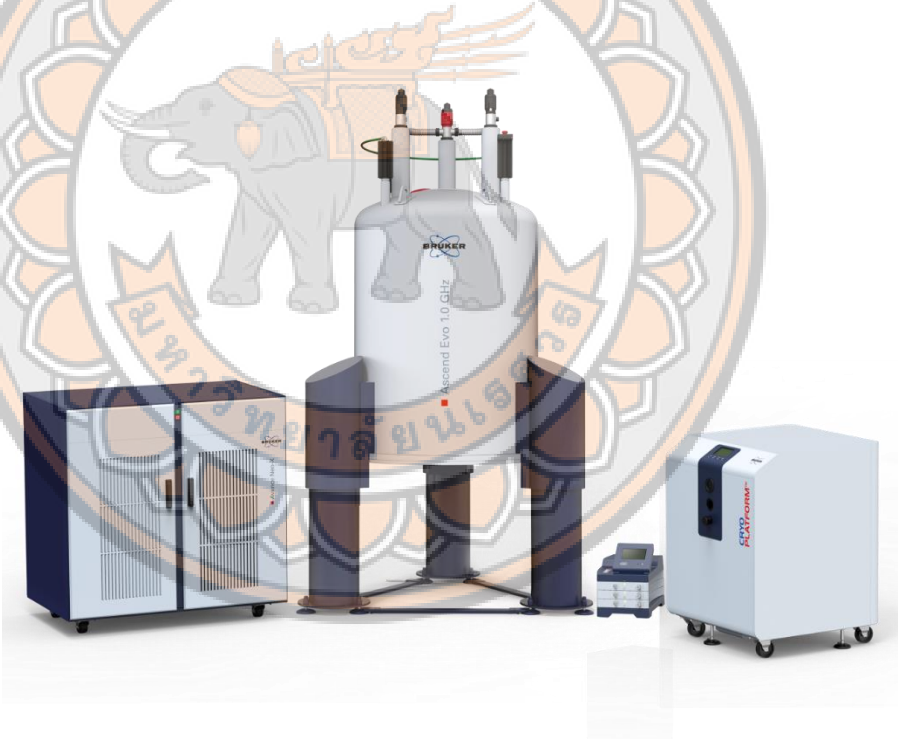

Figure 33 The 600 MHz Fourier Transform Nuclear Magnetic Resonance Spectrometer

Statistical analysis

The mean shear bond strength across the different experimental MDP concentrations was analyzed using one-way ANOVA followed by Tukey's post hoc test (SPSS version 20, IBM, Armonk, NY, USA). Failure modes were analyzed using the Chi-square test. The significance level for all analyses was set at $\alpha = 0.05$.

CHAPTER IV

RESULTS AND DISCUSSION

Part I: The difference of MDP concentrations

Shear bond strength

The means and standard deviations of the shear bond strength of all groups were shown in Table 3. The mean shear bond strength values of all groups in this study ranged from 3.7 to 11.3 MPa. The experimental 10% MDP group exhibited the highest mean shear bond strength, while the NMP group showed the lowest.

Group	SBS (Mpa)
2%	7.1 ± 0.4^{b}
4%	9.5 ± 1.4^{cd}
6%	10.4 ± 1.3^{de}
8%	10.4 ± 1.1^{de}
10%	11.3 ± 0.8^{e}
12%	7.6 ± 0.7^{b}
14%	7.7 ± 0.8^{bc}
NMP	3.7 ± 0.5^{a}
CMP	6.3 ± 1.0^{b}

Table 3 The means and standard deviations of shear bond strength of all groups

Mode of failure analysis

Table 4 displays the failure modes and mean percentage area of fracture for all specimens. Following the shear bond strength test, the failure mode of each experimental specimen was determined using a stereomicroscope (Olympus SZX2-ILLT, Tokyo, Japan) at ×20 magnification.

Experimental groups	Mode of failures					
	Adhesive	Cohesive	Mixed			
	n	*n*	*n*	Fracture in zirconia (%)	Fracture in composite resin (%)	Total (%)
NMP	6	0	0	0	0	0
CMP	0	0	6	0	16.4	16.4
2% MDP	0	0	6	0	25.8	25.8
4% MDP	0	0	6	0	29.2	29.2
6% MDP	0	0	6	0	48.4	48.4
8% MDP	0	0	6	0	68.1	68.1
10% MDP	0	0	6	0	73.2	73.2
12% MDP	0	0	6	0	35.2	35.2
14% MDP	0	0	6	0	34.0	34.0

Table 4 Mode of failures and means percentage of fracture of zirconia specimens *(n=6)*

Failures were classified into three categories: adhesive, cohesive, and mixed. Chi-square analysis indicated a significant difference in the incidence of mixed failure modes within the composite resin and the total sample.

In this study, all experimental MDP specimens fractured in the mixed failure mode. Cohesive failure was characterized by a fracture within the composite resin. Within the mixed failure mode, the percentage area of composite resin fracture ranged from 16.4% to 73.2%. The 10% MDP group exhibited the highest mean percentage area of resin fracture (73.2%), while the CMP group showed the lowest (16.4%). Conversely, the adhesive failure mode was predominantly observed in the NMP group.

Part II: FESEM

Surface characterization

Following the shear bond strength test, the surface characterization of the fractured specimens was examined using FESEM at 500× magnification. The failure modes were categorized into two types: adhesive failure and mixed failure.

According to the FESEM analysis, the sandblasted zirconia surface is shown in Figure 34A. The adhesive failure mode was observed in the NMP group (Figure 34B), whereas the mixed failure mode—combining adhesive failure with cohesive failure within the composite resin—was observed in the MDP-treated groups (Figure 34C). The surface characterization for all experimental groups is further illustrated in Figure 35.

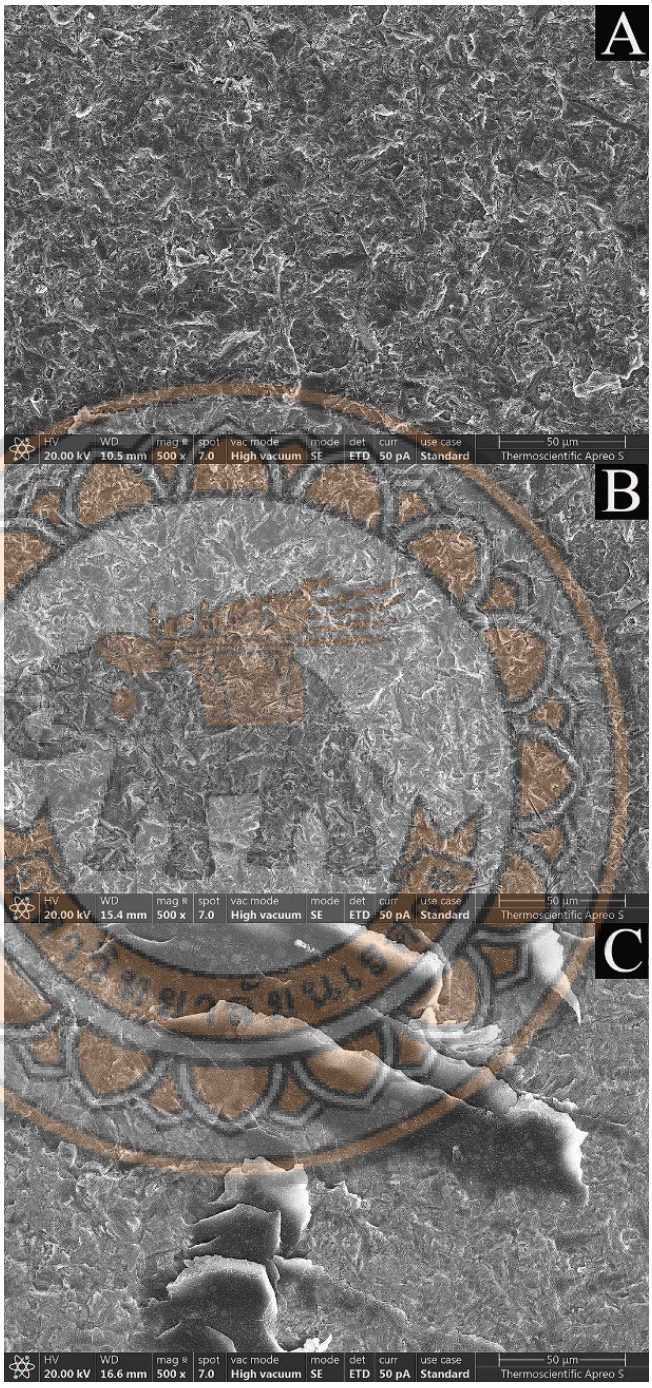

Figure 34 The representative 500× magnification of SEM images on the fracture surfaces of zirconia specimens. (A) The sandblasted zirconia surface, (B) The adhesive failure mode,

(C) The mixed failure mode

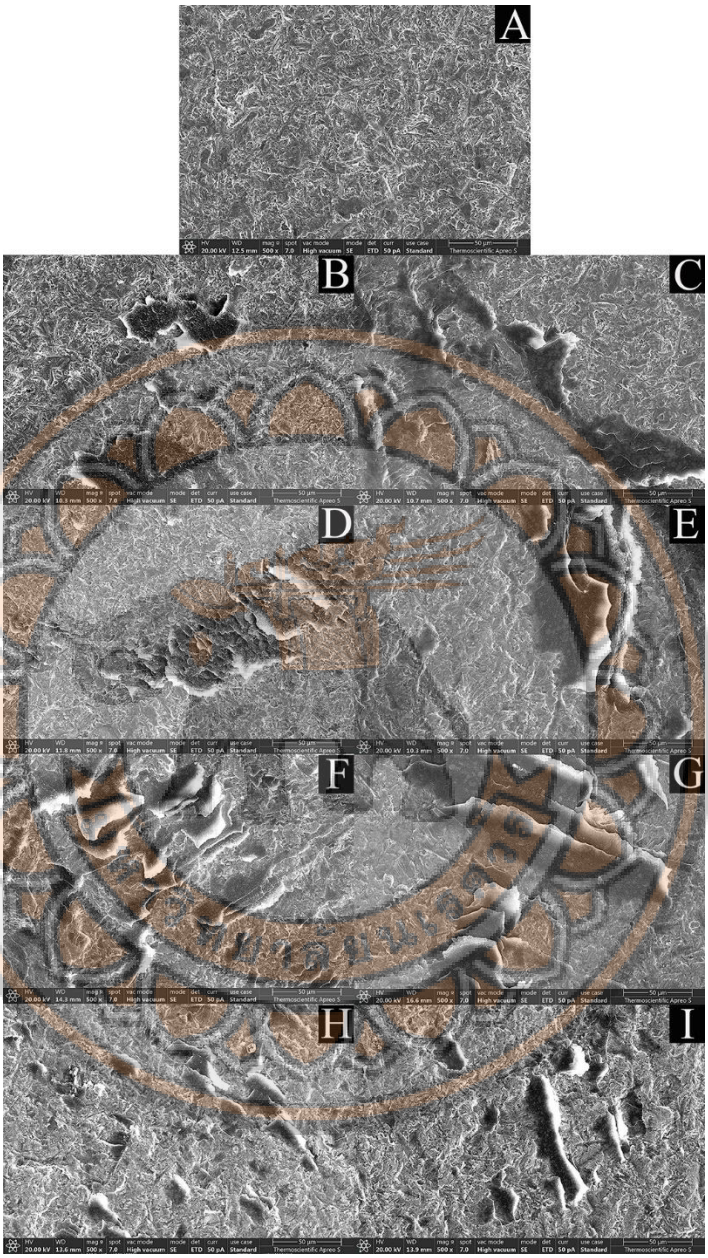

Figure 35 The representative 500× magnification of SEM images on the fracture surfaces of zirconia specimens for each group; (A) NMP group, (B) CMP group, (C) 2% MDP group,
(D) 4% MDP group, (E) 6% MDP group, (F) 8% MDP group, (G) 10% MDP group,
(H) 12% MDP group, (I) 14% MDP group

EDS on the fracture surface of the zirconia specimens

The atomic percentages of phosphorus (P) atoms on the fractured zirconia surfaces following the shear bond strength test are shown in Figure 36. The atomic percentage of carbon (C) atoms ranged from 0.0% to 1.5%. The atomic percentage of P atoms increased gradually, reaching a plateau in the 10% MDP group.

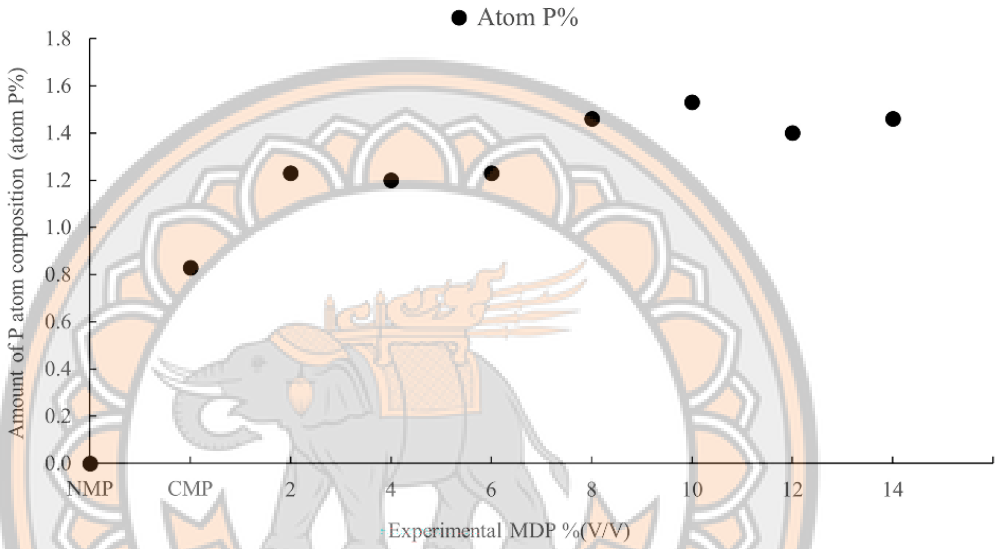

Figure 36 The amount of Phosphorus atom composition (atom P%) on the fracture surface of zirconia specimens in each group.

Part III: Molecular analysis

Solid State NMR of the zirconia specimens

The molecular interaction between the phosphate group and zirconia was investigated using solid-state NMR. Zirconia powder mixed with 2%, 4%, 10%, and 14% MDP was prepared for analysis, with untreated zirconia powder from the disc serving as a reference.

Figure 37 shows the ^{1}H NMR spectrum of untreated ZrO_2, where a major peaks at 4.81 ppm was observed. This peak was attributed to Zr–OH groups on the zirconia particles (8).

Liquid State NMR of MDP

The liquid-state ^{31}P NMR spectrum of MDP solution is also shown in Figure 37, exhibiting chemical shifts in the range of 1.77 to −10.82 ppm. Major peaks were observed at 0.59 ppm, which were attributed to the MDP monomer and are characteristic of phosphate groups; this confirms the presence of MDP in its expected molecular form. A sharp singlet at –10.82 ppm (MDP dimer) was also detected, possibly corresponding to a trace amount of fully deprotonated phosphate species or metal-complexed impurities (8, 17). Overall, this spectrum confirms the structural integrity of MDP as a phosphate monoester and verifies the presence of functional phosphate groups within the experimental MDP (18).

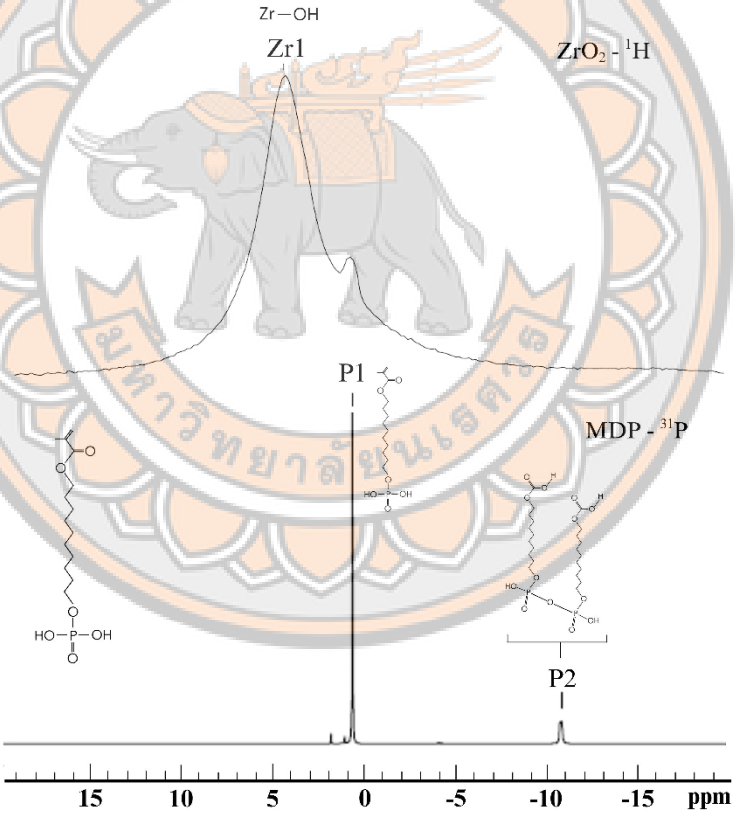

Figure 37 The ^{1}H NMR spectrum of ZrO_2 powder and the ^{31}P NMR spectrum of 10% MDP solution

DISCUSSION

Based on the results of this study, all groups treated with the MDP primer showed significantly higher shear bond strength compared to the NMP group. These findings suggest that MDP plays a crucial role in enhancing the bond between zirconia and composite resin, likely through chemical interactions at the zirconia interface that strengthen the bonding mechanism.

In the experimental MDP groups, the mean shear bond strength increased starting from the 2% MDP group, peaked at the 10% MDP group, and subsequently decreased in the 12% and 14% MDP groups. These results indicate that the shear bond strength between zirconia and composite resin does not have a direct linear correlation with the concentration of the MDP primer. Specifically, concentrations exceeding 10% MDP did not yield higher bond strengths. Therefore, a 10% MDP concentration was found to be the optimal concentration for use as a chemical surface treatment agent for zirconia.

Surface characterization of the fractured specimens in the NMP group revealed an adhesive failure mode (Figure 1B). In the absence of an MDP primer or adhesive agent, the composite resin failed to bond to the zirconia; consequently, only the sandblasted zirconia surface was visible, with no resin remnants remaining.

In contrast, the mixed failure mode—a combination of adhesive failure and cohesive failure within the composite resin—was observed in all MDP-treated groups (Figure 34C). The percentage of composite resin remnants varied across these groups, with the lowest coverage found in the CMP group (16.36%) and the highest in the 10% MDP group (73.23%). This percentage subsequently decreased in the 12% and 14% MDP groups to 35.22% and 33.98%, respectively. Notably, the trend in composite resin remnants correlated with the mean shear bond strength results, as higher bonding efficacy was directly associated with a greater amount of resin remaining firmly attached to the zirconia surface.

Following sandblasting treatment, FESEM imaging of the zirconia surface (Figure 38A) revealed a rough, irregular topography characterized by micropits, grooves, and

depressions. This increased surface roughness enhances micromechanical interlocking and provides a larger surface area for bonding with resin cement or primers (18).

The SEM image of the zirconia surface treated with the MDP primer (Figure 38B) shows a thin, continuous chemisorbed layer partially filling surface irregularities and adsorbing onto the sandblasted surface. Furthermore, the SEM image of the adhesive layer (Figure 38C) demonstrates a continuous film that covers and infiltrates the primer layer, producing a smoother and denser bonding interface.

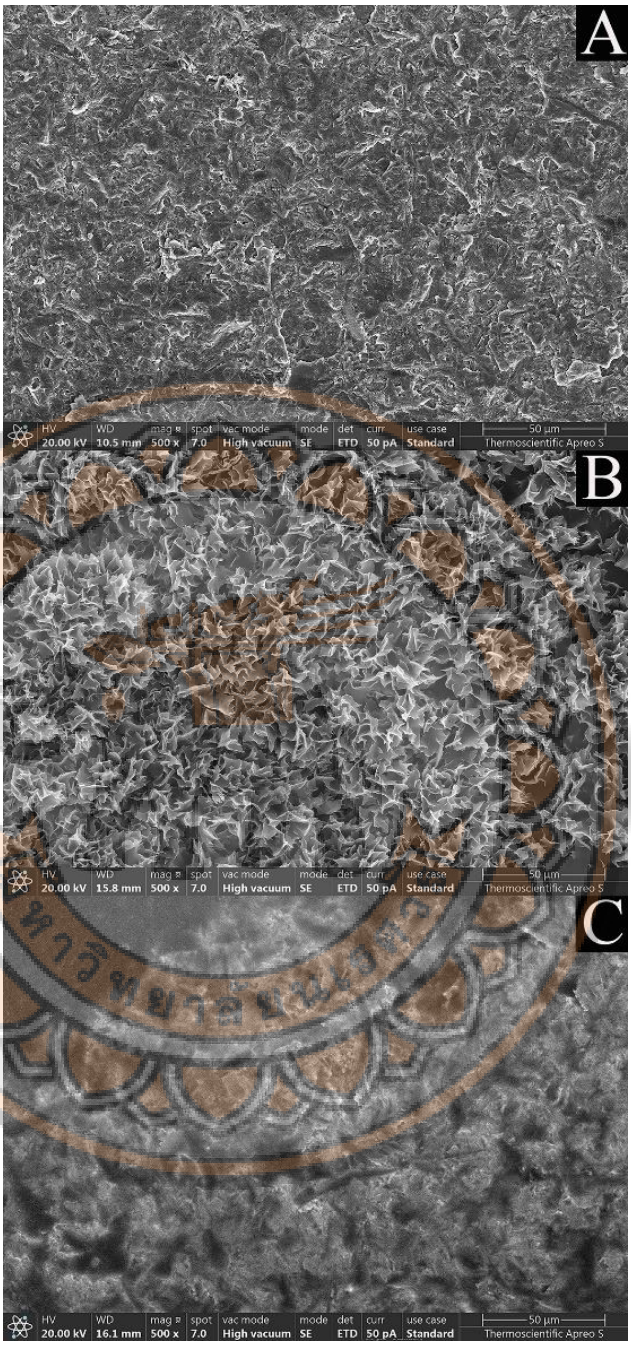

Figure 38 The representative 500× magnification of SEM images on the zirconia surfaces after surface treatment; (A) The sandblasted zirconia surface, (B) The sandblasted zirconia surface treated with MDP primer, (C) The sandblasted zirconia surface treated with MDP primer and adhesive agent

Based on the elemental analysis, the molecular structure of MDP contains C, H, O, and P, while the zirconia substrate consists of Zr and O. Because oxygen is found in both materials, it cannot be used to track their interaction. Therefore, phosphorus (P) was used as a marker to confirm that the MDP primer reached the bonding interface. However, the presence of phosphorus alone only proves that the MDP is there; it does not yet prove whether it has chemically bonded to the zirconia or is simply resting on the surface.

The amount of phosphorus (P) detected on the zirconia specimens was lowest in the CMP group (0.8 wt%). It increased through the 2%, 4%, and 6% MDP groups (1.2 wt%), rose further in the 8% MDP group (1.4 wt%), and reached its peak in the 10% MDP group (1.6 wt%). Subsequently, the P content slightly decreased to approximately 1.3–1.4 wt% in the 12% and 14% MDP groups.

The trend observed in the EDS analysis closely mirrored the shear bond strength patterns, indicating a strong correlation between the presence of phosphorus on the zirconia surface and the mean bond strength. Because these patterns are consistent, the phosphorus content measured by EDS may be associated with the quantity of chemical bonds formed between the phosphate functional groups (P–OH) of the MDP and the hydroxyl groups on the zirconia surface. Such chemical interactions play a critical role in enhancing interfacial adhesion between the zirconia and the composite resin. To verify whether a true chemical reaction occurred and to clarify the molecular configuration, NMR spectroscopy was employed.

The ^{1}H MAS NMR spectrum of untreated ZrO_2 powder, along with the ^{31}P MAS NMR spectrum of MDP in ethanol (ETH) solution, are shown in Figure 37. The spectrum of untreated ZrO_2 powder exhibits two major peaks: a prominent, broad peak at 4.81 ppm and a smaller peak at 1.16 ppm. Both correspond to the surface hydroxyl groups on the zirconium oxide particles, labeled Zr1 (11).

The ^{31}P MAS NMR spectrum of MDP in ETH solution also displays two peaks at 0.59 ppm and −10.82 ppm, labeled P1 and P2, which represent the monomeric and dimeric forms of MDP, respectively (19). This spectrum confirms the presence of phosphate groups in the MDP solution, these groups are chemically active and capable of forming bonds with metal oxides such as zirconia. These findings suggest that MDP has the potential to

chemically interact with the zirconia surface through its phosphate group, thereby enhancing bond strength and improving the stability of the interface.

The ^{31}P NMR spectrum of the mixture containing zirconia powder and 10% MDP solution (labeled as Z10 in Figure 39) captures the primary chemical shifts identified in this study through five distinct peaks, labeled S1 to S5. The S1 peak, located at –1.28 ppm, corresponds to MDP monomers adsorbed onto the zirconia surface via hydrogen bonding. The S2 peak at –7.03 ppm is attributed to monodentate phosphate–zirconia complexes adsorbed through ionic bonding; these are further stabilized by inter-complex hydrogen bonding to form a bidentate configuration. Meanwhile, the S3 peak at –12.89 ppm is assigned to a phosphate group bridging two zirconium atoms through a combination of hydrogen and ionic bonding. Finally, the S4 and S5 peaks, found at –19.43 and –21.58 ppm, respectively, are likely representative of oligomers formed via covalent interactions between multiple phosphate groups (8,20).

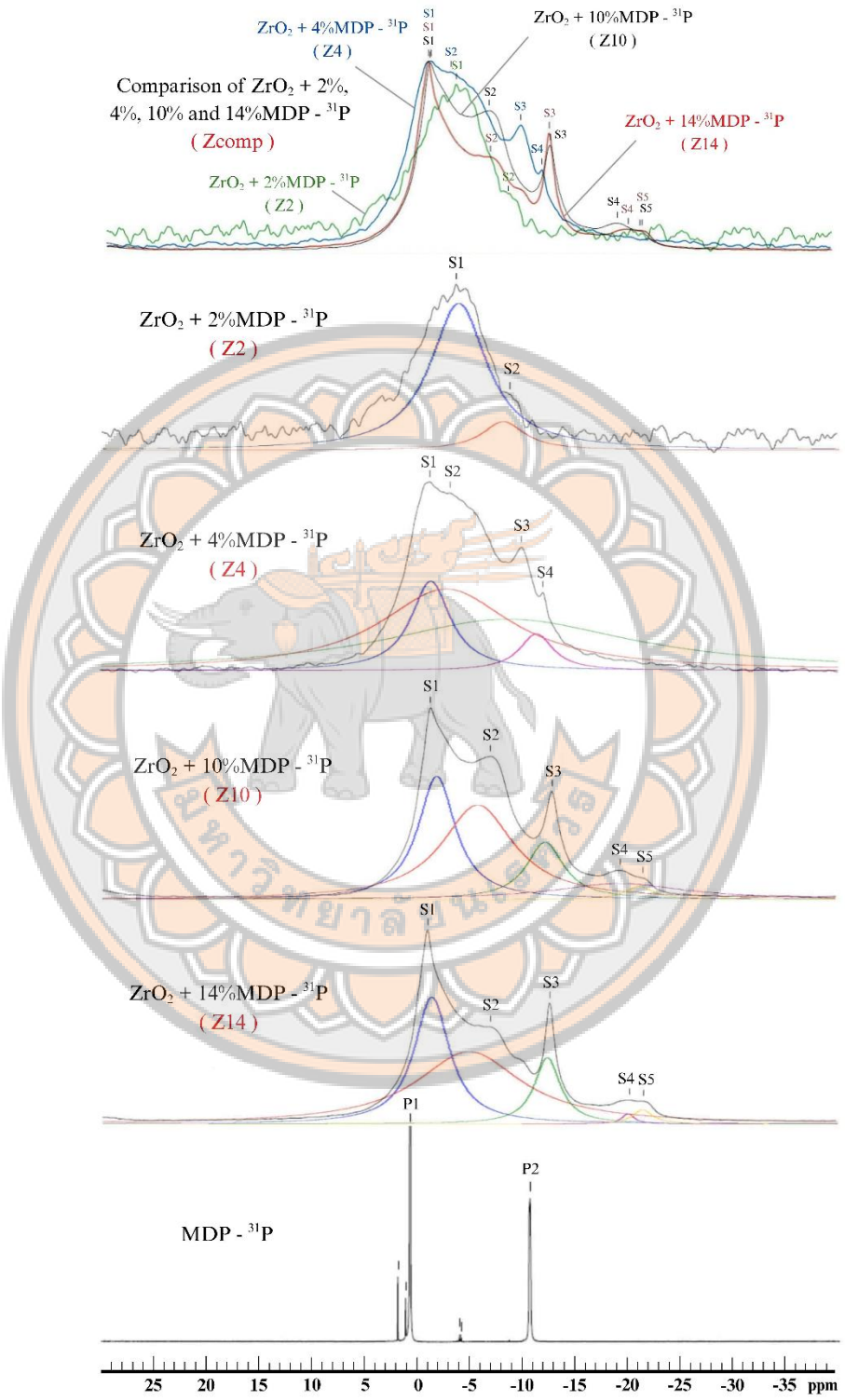

Figure 39 The comparison of ^{31}P NMR spectra of Z2, Z4, Z10 and Z14, the ^{31}P NMR spectra of Z2, Z4, Z10, Z14 and 10% MDP solution

These identified chemical shifts (Zr1, P1–P2, and S1–S5) provide a comprehensive profile of the molecular interactions at the interface. By correlating these specific peaks with their corresponding proposed chemical structures, as illustrated in Figure 40, the transition from simple physical adsorption to complex chemical bonding is clearly demonstrated. This progression highlights how the different coordination modes of the phosphate group contribute to the overall stability and strength of the zirconia–resin bond.

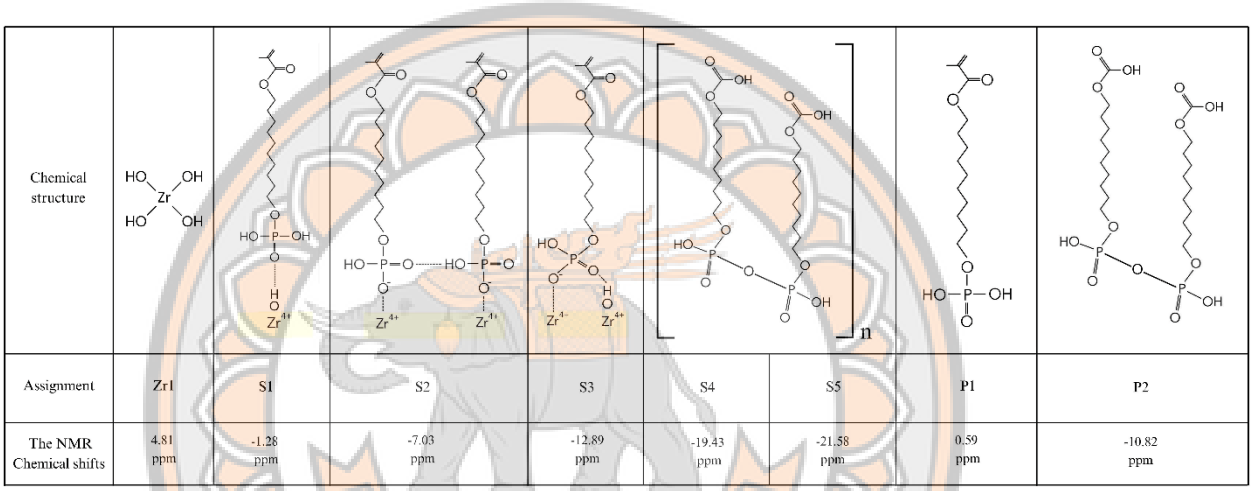

Figure 40 The representative of the assignment of the ^{1}H NMR spectrum of pure zirconia, the ^{31}P NMR spectrum of 10% MDP solution and the ^{31}P NMR spectra of the mixture of zirconia powder + 10% MDP solution

Figure 39 presents the ^{31}P NMR spectra of zirconia powder treated with 2%, 4%, 10%, and 14% MDP solutions— subgroups identified as Z2, Z4, Z10, and Z14, respectively. These subgroups were selected for detailed analysis as they represent the range of concentrations that exhibited no significant statistical differences in shear bond strength. In addition to the primary spectra, the figure includes the deconvoluted peaks for each subgroup, a comparative spectrum labeled Zcomp, and the baseline ^{31}P NMR spectrum of the 10% MDP solution for reference. As observed, the chemical shift peaks varied among the groups according to the MDP concentration, indicating that the nature of the phosphate–zirconia interactions is concentration-dependent.

Peak deconvolution was utilized to separate overlapping signals and reveal hidden individual components (16). The deconvoluted peaks are displayed as colored lines beneath the black aggregate spectrum: blue for S1, red for S2, green for S3, pink for S4, and yellow for S5. While the spectral patterns of the Z2, Z10, and Z14 groups aligned well with their respective deconvoluted peaks, this was not observed for the Z4 group.

In the Z4 spectrum, the primary signal appeared as a broad, intense peak where the S1 and S2 components were positioned in very close proximity. Due to this overlap, the apparent intensity of S1 and S2 in the aggregate spectrum could not be considered reliable. Instead, the two signals merged into a single broad peak with shoulder points at the S1 and S2 positions. Consequently, the true intensities of the S1 and S2 peaks in the Z4 group should be evaluated based on the deconvoluted components rather than the raw aggregate spectrum.

Figure 39 (Zcomp) compares the ^{31}P NMR spectra of the Z2, Z4, Z10, and Z14 groups. Peaks S1 and S2 were detected across all groups, although only the S1 peak and a low-intensity S2 peak were observed in the Z2 group. In the Z4, Z10, and Z14 groups, the intensity of the S1 peak was relatively consistent and notably higher than that of the Z2 group.

In contrast, the intensity of the S2 peak varied significantly: it was highest in the Z10 group, followed by Z4 and Z14, and lowest in Z2. The S3 peak followed an opposite trend, exhibiting its highest intensity in Z14, followed by Z10, and its lowest in Z4; it was entirely absent in the Z2 group. Finally, the S4 and S5 peaks were detected only in the Z10 and Z14 groups, with no significant differences in intensity observed between them.

Regarding the relationship between the chemical shifts and bond strength, the highest bond strength was achieved in the Z10 group, followed by Z14, Z4, and finally Z2. This trend corresponded to the number of peaks observed in each group— specifically, a greater variety of chemical shifts correlated with higher bond strength. The Z2 group, where only the S1 peak and a low-intensity S2 peak were detected, exhibited the lowest bond strength. This suggests that the predominant presence of the S1 peak, with only a minor contribution from S2, is insufficient to achieve high and stable bond strength, likely due to the low concentration of the MDP solution.

The S1 peak represents MDP monomers adsorbed via hydrogen bonding, whereas the S2 peak corresponds to two MDP monomers bridged through hydrogen bonding and interacting with zirconia via ionic bonding. Based on these observations, it is likely that the initial interaction between MDP and zirconia is characterized by hydrogen bonding (S1), which then facilitates the formation of ionic bonds (S2) as concentration increases.

The Z4 group exhibited increased bond strength, characterized by the presence of peaks S1, S2, and S3. Compared to the Z2 group, Z4 showed higher intensities for both the S1 and S2 peaks. The higher concentration of the MDP solution allowed a greater number of phosphate groups to interact with the zirconia surface; this resulted not only in the increased intensities of S1 and S2 but also in the emergence of the S3 peak. These additional phosphate groups likely bonded to zirconium atoms through combined hydrogen and ionic interactions, directly corresponding to the enhanced intensity of the S3 signal.

While the ^{31}P NMR spectra of both the Z10 and Z14 groups contained all identified chemical shifts, the highest bond strength was observed in the Z10 group. A comparison of the two groups reveals that while the intensity of the S1 peak was similar, the S2 peak in Z10 was approximately twice as intense as in Z14. Meanwhile, the intensities of the S3, S4, and S5 peaks remained nearly identical between the two groups.

Based on these spectral profiles and the corresponding shear bond strengths, it appears that the intensities of S3, S4, and S5 are not directly correlated with bond stability or strength. In contrast, the superior bond strength of the Z10 group corresponds directly to its significantly higher S2 peak intensity. From this observation, it can be concluded that the S2 peak—attributed to ionic bonding—represents a bonding configuration that plays a dominant role in enhancing adhesion. This configuration provides a greater contribution to bond strength than the hydrogen bonding associated with the S1 and S3 peaks.

Based on the chemical structures of S1, S2, and S3, the S1 configuration is defined as a monodentate phosphate–zirconia complex bonded via hydrogen bonding, characterized as a "one-by-one" configuration. In contrast, the S2 configuration consists of two monodentate complexes where each phosphate group bonds to a separate zirconium atom through ionic bonding, further stabilized by inter-molecular hydrogen bonding in a "double one-by-one" configuration; this arrangement facilitates a robust bond both to the zirconia

surface and between adjacent MDP molecules. The S3 configuration involves a single phosphate group bridging two zirconium atoms through one ionic and one hydrogen bond, creating a "one-to-two" configuration (8). These bonding modes are distinct, and as phosphate groups populate the zirconia surface, their molecular tails may cause crowding or obstructing adjacent groups. Consequently, additional phosphate groups may be prevented from approaching the surface closely enough to form direct chemical bonds. Instead, these non-bonding groups likely overlap in subsequent layers to form phosphate oligomers, which are represented by the S4 and S5 peaks.

Due to the crowding of their extended molecular tails and close proximity, these phosphate groups were unable to bond to the zirconia surface or position themselves efficiently. Instead, they were forced to shift away from existing groups or rotate into alternative orientations to fit within the available space. Consequently, bonding area became limited, and the zirconia surface was not fully utilized. This phenomenon likely stemmed from the imbalance in the ratio of S1, S2, and S3 configurations. An excessive number of S1 and S3 configurations may occupy disproportionate surface area and obstruct the formation of the S2 configuration, leading to a decrease in S2 intensity even as S1 and S3 intensities increase.

This ratio appears to be directly influenced by the concentration of the MDP solution. At an optimal concentration, the number of phosphate groups produces a balanced ratio of S1, S2, and S3 configurations with the highest possible proportion of S2, thereby achieving the maximum bond strength between the MDP and the zirconia surface.

Increasing the MDP concentration eventually creates an environment characterized by an excess of monomers and phosphate oligomers, resulting in to the formation of multilayers. The optimal concentration of the MDP solution produces an appropriate ratio of S1, S2, and S3 configurations that efficiently occupy the available surface bonding sites. Once these sites reach saturation, additional phosphate groups can no longer interact directly with the zirconia surface; therefore, increasing the MDP concentration beyond this threshold is unnecessary. Overall, a 10% MDP concentration appears to provide the most balanced and suitable coordination profile before saturation or molecular overcrowding effects become significant.

The chemical shifts observed in the ^{31}P NMR spectra of zirconia mixed with various concentrations of MDP provide clear evidence of chemical interactions at the interface. These results offer valuable insight into the specific concentrations that promote optimal bonding. The interactions, including hydrogen and ionic bonding, result in distinct peaks that represent unique coordination configurations. This NMR evidence, supported by EDS analysis, confirms the presence of chemical bonding between MDP and zirconia, which likely drives the improved bond strength between the zirconia and the resin composite (21).

CHAPTER V

CONCLUSIONS

Within the limitations of this study, it was concluded that MDP can directly bond to the zirconia surface via chemical bonds, including ionic bonds and hydrogen bonds, which was confirmed by the ^{31}P solid-state NMR spectra of the mixture of zirconia and various concentrations of MDP. The mean shear bond strength between zirconia and composite resin did not increase further with MDP concentration beyond 10% MDP due to the saturation and overcrowding of the bonding surface area. The 10% MDP was the optimal concentration to achieve the greater chemical bonding environment, which resulted in the highest shear bond strength between zirconia and composite resin.

REFERENCES

REFERENCES

1. Al-Amari AS, Saleh MS, Albadah AA, et al. A Comprehensive Review of Techniques for Enhancing Zirconia Bond Strength: Current Approaches and Emerging Innovations. Cureus 2024;16(10):e70893.

2. Gomes AL, Castillo-Oyagüe R, Lynch CD, Montero J, Albaladejo A. Influence of sandblasting granulometry and resin cement composition on microtensile bond strength to zirconia ceramic for dental prosthetic frameworks. J Dent 2013;41(1):31-41.

3. Valente F, Mavriqi L, Traini T. Effects of 10-MDP Based Primer on Shear Bond Strength between Zirconia and New Experimental Resin Cement. Materials (Basel) 2020;13(1):235.

4. Wongkamhaeng K, Poomparnich K, Chitkraisorn T, Boonpitak K, Tosiriwatanapong T. Effect of combining different 10-MDP-containing primers and cement systems on shear bond strength between resin cement and zirconia. BMC Oral Health 2025;25:206.

5. Abhishek G, Vishwanath SK, Nair A, Prakash N, Chakrabarty A, Malalur AK. Comparative evaluation of bond strength of resin cements with and without 10-methacryloyloxydecyl dihydrogen phosphate (mdp) to zirconia and effect of thermocycling on bond strength - An in vitro study. J Clin Exp Dent 2022;14(4):e316-e320.

6. Grégoire G, Coppel Y, Payre B, Tavernier B. Chemical interaction of a self-adhesive resin cement with zirconia studied by solid-state NMR spectroscopy and energy dispersive X-ray microanalysis. Oral Health and Care 2023;8:1-7.

7. Shin J, Lim MH, Han J. NMR spectroscopic investigations of transition metal complexes in organometallic and bioinorganic chemistry. Bull Korean Chem Soc 2024;45(7):593-613.

8. Nagaoka N, Yoshihara K, Feitosa VP, et al. Chemical interaction mechanism of 10-MDP with zirconia. Sci Rep 2017;7:45563.

9. Yue X, Hou X, Gao J, Bao P, Shen J. Effects of MDP-based primers on shear bond strength between resin cement and zirconia. Exp Ther Med 2019;17(5):3564-72.

10. Shibuya K, Ohara N, Ono S, Matsuzaki K, Yoshiyama M. Influence of 10-MDP concentration on the adhesion and physical properties of self-adhesive resin cements. Restor Dent Endod 2019;44(4):e45.

11. Yoshida K. Effect of 10-Methacryloyloxydecyl Dihydrogen Phosphate Concentrations in Primers on Bonding Resin Cements to Zirconia. J Prosthodont 2021;30(4):356-62.

12. Chen Y, Lu Z, Qian M, Zhang H, Xie H, Chen C. Effect of 10-Methacryloxydecyl Dihydrogen Phosphate Concentration on Chemical Coupling of Methacrylate Resin to Yttria-stabilized Zirconia. J Adhes Dent 2017;19(4):349-55.

13. Calamita RS, Oliveira AAD, Pizzanelli GG, et al. Interaction of different concentrations of 10-MDP and GPDM on the zirconia bonding. Dent Mater 2023;39(7):665-8.

14. Kim H-K, Yoo K-W, Kim S-J, Jung C-H. Phase Transformations and Subsurface Changes in Three Dental Zirconia Grades after Sandblasting with Various Al2O3 Particle Sizes. Materials 2021;14:5321.

15. Zhao Q, Han F, Yuan X, Chen C. Effects of Solvents and pH Values on the Chemical Affinity of 10-Methacryloyloxydecyl Dihydrogen Phosphate toward Hydroxyapatite. ACS Omega. 2021;6(29):19183-93.

16. Borisov A, Hazendonk P, Hayes P. 31 P MAS NMR Spectroscopy of Hexachlorocyclotriphosphazene at Different Stages During Thermal Ring-Opening Polymerization. J Inorg Organomet Polym Mater. 2010;20:395-8.

17. Yoshihara K, Nagaoka N, Okihara T, et al. Functional monomer impurity affects adhesive performance. Dent Mater. 2015;31(12):1493-501.

18. Prasad HA, Pasha N, Hilal M, Amarnath GS, Kundapur V, Anand M, et al. To Evaluate Effect of Airborne Particle Abrasion using Different Abrasives Particles and Compare Two Commercial Available Zirconia on Flexural Strength on Heat Treatment. Int J Biomed Sci. 2017;13(2):93-112.

19. Fukegawa D, Hayakawa S, Yoshida Y, Suzuki K, Osaka A, Van Meerbeek B. Chemical interaction of phosphoric acid ester with hydroxyapatite. J Dent Res. 2006;85(10):941-4.

20. Godinot C, Gaysinski M, Thomas OP, Ferrier-Pagès C, Grover R. On the use of 31P NMR for the quantification of hydrosoluble phosphorus-containing compounds in coral host tissues and cultured zooxanthellae. Sci Rep. 2016;6:21760.

21. Ieamsuwantada T, Yamockul S, Thamrongananskul N, Surintanasarn A, Klaisiri A. The Effect of Cement Thickness on Shear Bond Strength of Zirconia with Three Different Self-Adhesive Resin Cements. Eur J Dent. 2025;19(4):948-55.